

# Semantic Refinement with LLMs for Graph Representations

Safal Thapaliya<sup>1,\*</sup>, Zehong Wang<sup>2,\*</sup>, Jiazheng Li<sup>1</sup>, Ziming Li<sup>1</sup>, Yanfang Ye<sup>2</sup>, Chuxu Zhang<sup>1,†</sup>

<sup>1</sup>University of Connecticut, USA <sup>2</sup>University of Notre Dame, USA

{safal.thapaliya, jiazheng.li, ziming.li, chuxu.zhang}@uconn.edu, {zwang43, yye7}@nd.edu

\*Equal Contribution †Corresponding Author

## Abstract

Graph-structured data exhibit substantial heterogeneity in where their predictive signals originate: in some domains, node-level semantics dominate, while in others, structural patterns play a central role. This structure-  
semantics heterogeneity implies that no graph learning model with a fixed inductive bias can generalize optimally across diverse graph domains. However, most existing methods address this challenge from the model side by incrementally injecting new inductive biases, which remains fundamentally limited given the open-ended diversity of real-world graphs. In this work, we take a data-centric perspective and treat node semantics as a task-adaptive variable. We propose a **Data-Adaptive Semantic Refinement** framework (**DAS**) for graph representation learning, which couples a fixed graph neural network (GNN) and a large language model (LLM) in a closed feedback loop. The GNN provides implicit supervisory signals to guide the semantic refinement of LLM, and the refined semantics are fed back to update the same graph learner. We evaluate our approach on both text-rich and text-free graphs. Results show consistent improvements on structure-dominated graphs while remaining competitive on semantics-rich graphs, demonstrating the effectiveness of data-centric semantic adaptation under structure-  
semantics heterogeneity.

## 1 Introduction

Graph-structured data (Wu et al., 2020; Zhang et al., 2020) are ubiquitous in the real world, arising in diverse domains such as citation networks, social platforms, molecular interaction systems, and transportation infrastructures. Despite sharing the same graph abstraction, these domains differ fundamentally in where their predictive signals originate. In citation networks, for example, each node represents a scientific document whose topical content and research focus are explicitly encoded in natural

language. Here, node-level semantics—captured by titles, abstracts, or full texts—often provide the primary discriminative signal for downstream tasks, while citation links mainly serve as a contextual scaffold that propagates and regularizes semantic information (Greenberg, 2009; Zhao and Strotmann, 2015; Zhang et al., 2019b). By contrast, in domains such as molecular graphs or transportation networks, semantic attributes are weak or even absent (Wu et al., 2018). Instead, node identity and functionality are determined predominantly by structural roles and global topological patterns, such as motifs, connectivity configurations, and relative positional relationships (Chen et al., 2020; Zhang et al., 2024a; Wang et al., 2025c). These examples demonstrate that predictive signals in real-world graphs may be dominated by semantics, dominated by structure, or arise from their intricate interplay.

This observation leads to a fundamental and unavoidable consequence: *the balance between semantics and structure is inherently domain-dependent, rather than governed by a universal principle*. As a result, no graph learning model with a fixed inductive bias can perform optimally across graph domains with drastically different structure-  
semantics regimes (Platonov et al., 2023).

However, translating this observation into a practical learning system remains challenging. For a new graph, the dominant source of predictive signal—whether driven by semantics, structure, or their interaction—is unknown a priori, yet both the model and the data representation must commit to specific inductive biases in advance. Modern GNNs encode fixed architectural preferences once chosen, favoring, for example, locality (Veličković et al., 2018), long-range dependencies (Xu et al., 2019; Rampášek et al., 2022), or substructure information (Wang et al., 2025b,d). Meanwhile, node representations—whether feature vectors (Kipf and Welling, 2017), textual embeddings (Wang et al.,

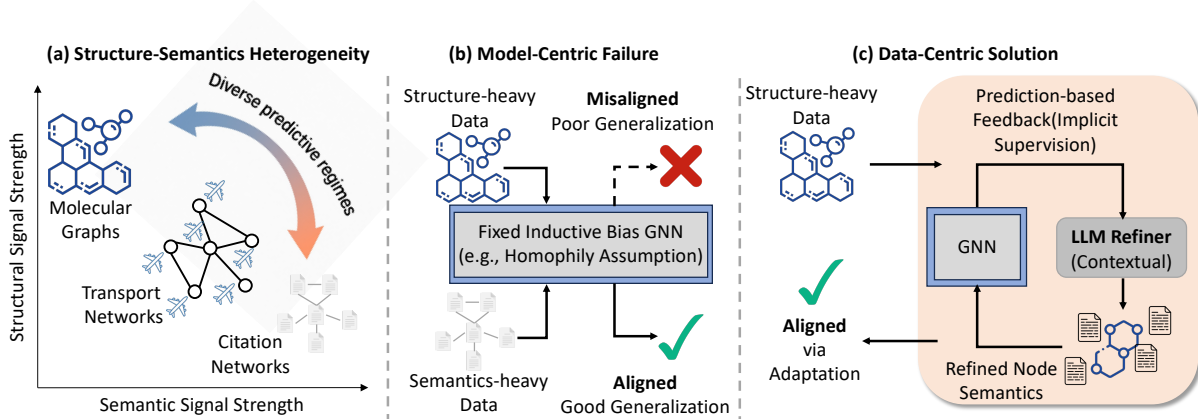


Figure 1: **Structure–semantic heterogeneity and data-centric adaptation.** (a) Real-world graphs vary widely in their reliance on semantic and structural patterns as sources of predictive signal. (b) Model-centric approaches with fixed inductive biases become misaligned when deployed across graphs with different structure–semantic regimes, leading to poor generalization. (c) In contrast, our proposed DAS keeps the graph model fixed and iteratively refines node semantics through prediction-driven feedback, adapting the data representation to the target task.

2024b), or structural descriptors (Perozzi et al., 2014; Grover and Leskovec, 2016)—are typically constructed in a predefined manner and kept fixed throughout training. As a result, the learning system becomes implicitly specialized to a particular structure–semantic regime. When this specialization is mismatched with the true signal distribution of the target graph, performance degrades systematically, and adaptation in practice is often reduced to empirical model and feature selection rather than a principled mechanism.

To balance semantics and structure, most existing methods approach this problem primarily from the model side. One line of work adapts GNN architectures by redesigning message passing (Morris et al., 2019; Zhang et al., 2019a; Fan et al., 2022), incorporating adaptive aggregation (Ying et al., 2018), or injecting positional encodings (Murphy et al., 2019), thereby embedding different inductive biases into the model. Beyond architectural modifications, another line of work introduces external reasoning models (Chen et al., 2024b; Wang et al., 2023a), most notably large language models (LLMs) (Zhao et al., 2023b; Ye et al., 2025), which process graph structures and node attributes in textual form. In parallel, other methods rely on auxiliary models (Chen et al., 2024b) to generate additional semantic signals—such as synthetic attributes (He et al., 2023)—that are subsequently consumed by a downstream GNN. Despite their empirical success, these approaches fundamentally rely on incrementally injecting model-level inductive biases, which cannot guarantee universal adaptability across open-ended and structurally diverse

graph domains.

In this work, we take a fundamentally different stance on structure–semantic heterogeneity by shifting the adaptation from the model to the data. Instead of continually expanding model-level inductive biases, we treat node semantics as a task-adaptive variable. This shift is motivated by the observation that the balance between structure and semantics is ultimately realized through the input representations consumed by the model, rather than through the architecture alone. As a result, misalignment on new graph domains often arises from fixed node semantics that fail to reflect the graph-specific source of predictive signal.

Building on this perspective, we propose **Data-Adaptive Semantic Refinement (DAS)**, a data-centric, feedback-driven framework for iterative semantic adaptation. Starting from initial node descriptions or structure-derived verbalizations (Wang et al., 2025a), we train a fixed GNN for the downstream task and use its predictions as implicit supervision. A large language model then refines node semantics by conditioning on both structural context and model behavior, and the refined descriptions are fed back to update the same graph learner. By iterating this closed loop for a small number of rounds, DAS progressively aligns node semantics with the structure–semantic regime of the target graph without modifying the underlying model. We evaluate DAS on both text-attributed and text-free graphs, where it consistently improves performance on structure-dominated graphs while remaining competitive on semantics-rich graphs.

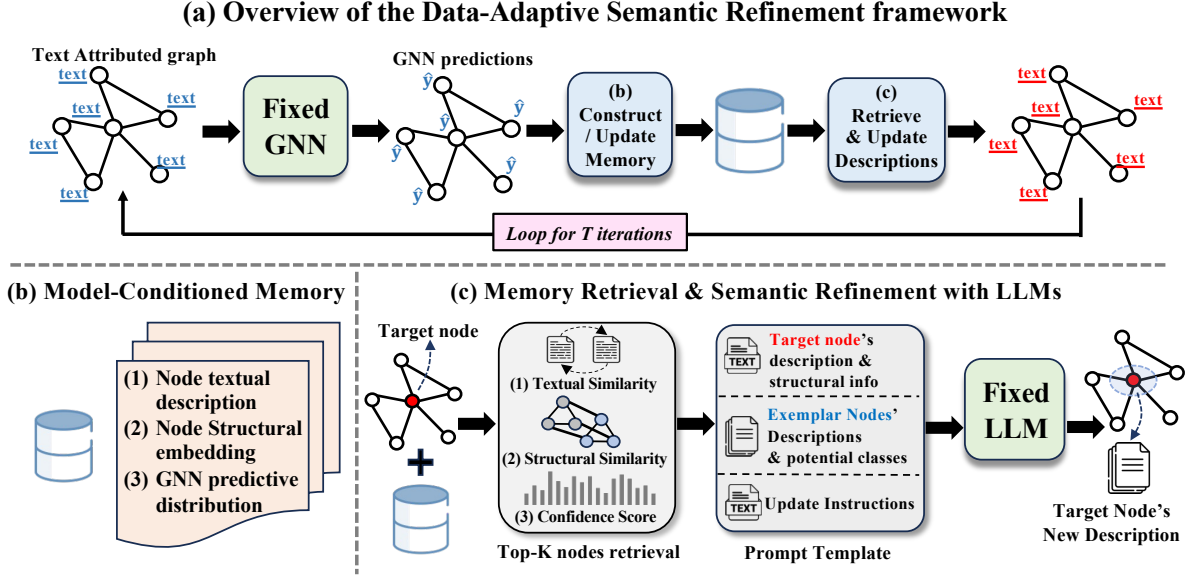


Figure 2: **Overview of the DAS framework.** Node descriptions are iteratively refined through a closed loop between a fixed GNN and an LLM. At each iteration, the GNN provides task feedback and a model-conditioned memory retrieves structurally and semantically aligned in-graph exemplars, which guide the LLM to update node semantics before feeding them back to the same GNN.

## 2 Methodology

### 2.1 Problem Definition

We consider a graph  $G = (\mathcal{V}, \mathcal{E})$  with node set  $\mathcal{V}$  and edge set  $\mathcal{E}$ . Each node  $v \in \mathcal{V}$  is associated with an initial description  $r_v$ , which is either a natural language text (in text-attributed graphs) or a structure-derived verbalization (in text-free graphs). A subset of nodes  $\mathcal{V}_{\text{train}} \subseteq \mathcal{V}$  is labeled with  $y_v \in \mathcal{Y}$ . Given a GNN  $g_\theta$  for node classification, we treat node semantics as adaptive variables. Our objective is to iteratively refine node descriptions  $\{d_v\}_{v \in \mathcal{V}}$  from the initial inputs  $\{r_v\}$ , such that the refined semantics better align with both the graph structure and the downstream prediction task. After  $T$  refinement steps, the final classifier  $g_\theta$  trained on  $\{d_v^{(T)}\}$  is used for evaluation.

### 2.2 Overview

DAS is a data-centric, feedback-driven framework that adapts node semantics under structural context and task supervision while keeping the graph model fixed. Instead of modifying model architectures to handle heterogeneous structure–semantics regimes, DAS treats node descriptions as adaptive states that are iteratively refined through a closed loop between a GNN and an LLM.

As illustrated in Figure 2, DAS operates over  $T$  refinement iterations. At iteration  $t$ , each node  $v \in \mathcal{V}$  is associated with a description  $d_v^{(t)}$  (initialized

as  $d_v^{(0)} = r_v$ ), which is encoded into node features and fed into a fixed GNN  $g_\theta$  to produce predictions

$$\mathbf{p}_v^{(t)} = g_\theta(\mathbf{x}_v^{(t)}, G). \quad (1)$$

The current descriptions and predictions are stored in a history buffer  $\mathcal{B}^{(t)}$ , from which an in-graph support set  $\mathcal{S}_v^{(t)}$  is retrieved for each node. Conditioned on  $d_v^{(t)}$  and  $\mathcal{S}_v^{(t)}$ , the LLM refines the node semantics as

$$d_v^{(t+1)} = \mathcal{M}(d_v^{(t)}, \mathcal{S}_v^{(t)}). \quad (2)$$

The refined descriptions are then fed back to the same GNN, completing one refinement iteration.

Through this feedback-driven loop, DAS progressively aligns node semantics with the structure–semantics regime of the target graph. Unlike prior LLM-enhanced methods that rely on fixed prompts or exemplars (He et al., 2023; Chen et al., 2024b; Wang et al., 2025a), DAS enables task-conditioned semantic evolution guided by model behavior.

### 2.3 Structure-Aware Initial Node Semantics

We construct initial node descriptions by expressing structural information in natural language, so that both semantic and structural cues can be processed in a unified textual space. Following Wang et al. (2025a), for each node  $v \in \mathcal{V}$  we compute a small set of structural statistics, including degree, betweenness, closeness, clustering coefficient, and

square clustering coefficient (Zhang and Luo, 2017; Saramäki et al., 2007; Zhang et al., 2008). We present a detailed discussion in Appendix C.

To eliminate scale variation across graphs, each statistic is converted into a percentile rank within the graph. These normalized values are then mapped into a concise structural summary  $t_v^{\text{struct}}$  via a fixed template, as shown in Appendix I. For text-attributed graphs, we set  $d_v^{(0)} = [r_v \parallel t_v^{\text{struct}}]$ , while for text-free graphs we use  $d_v^{(0)} = t_v^{\text{struct}}$ . This design expresses both semantic and structural information in a single textual modality, enabling consistent encoding and subsequent refinement.

## 2.4 Model-Conditioned Memory

We maintain a model-conditioned memory to explicitly represent how node semantics, graph structure, and task predictions interact during each refinement stage. At iteration  $t$ , the memory is denoted as  $\mathcal{B}^{(t)} = \{\beta_v^{(t)}\}_{v \in \mathcal{V}}$ , which stores node-level states induced by the current descriptions  $\{d_v^{(t)}\}$  under the fixed GNN  $g_\theta$ . For each node  $v \in \mathcal{V}$ , the memory stores a joint state triple

$$\beta_v^{(t)} = (d_v^{(t)}, \mathbf{s}_v, \mathbf{p}_v^{(t)}), \quad (3)$$

where  $d_v^{(t)}$  is the current textual description,  $\mathbf{s}_v$  denotes a structure-oriented embedding encoding the node’s topological role via `struc2vec` (Ribeiro et al., 2017), and  $\mathbf{p}_v^{(t)}$  is the predictive distribution produced by the GNN. This triple defines a semantic–structural–predictive state for each node under the current representation.

**Memory Construction and Update.** At  $t = 0$ , the initial memory  $\mathcal{B}^{(0)}$  is constructed from the initial descriptions  $\{d_v^{(0)}\}$ , the fixed structural embeddings  $\{\mathbf{s}_v\}$ , and the GNN predictions obtained using these features. At each subsequent iteration  $t > 0$ , the descriptions are updated to  $\{d_v^{(t)}\}$ , re-encoded as node features, and fed into the same GNN. The resulting predictive states  $\{\mathbf{p}_v^{(t)}\}$  are then used to overwrite the previous memory entries, yielding an updated memory  $\mathcal{B}^{(t)}$ . This rolling update scheme ensures that the memory always reflects the latest alignment between node semantics, graph structure, and task-specific behavior.

**Memory Retrieval.** Given the memory  $\mathcal{B}^{(t)}$ , the goal of memory retrieval is to identify, for each target node  $v$ , a small set of in-graph exemplars  $\mathcal{S}_v^{(t)}$  that are simultaneously *semantically relevant*,

*structurally aligned*, and *reliable under the current classifier*. These exemplars serve as task-aware references for subsequent semantic refinement.

To this end, the memory induces a joint semantic–structural similarity space. Let  $\mathbf{t}_v^{(t)}$  denote the embedding of the current description  $d_v^{(t)}$  produced by the text encoder (Wang et al., 2020), and let  $\mathbf{s}_v$  denote the structural embedding encoding the topological role of node  $v$ . For any pair of nodes  $(v, u)$ , we define the semantic similarity

$$\text{sim}_t(v, u) = \frac{(\mathbf{t}_v^{(t)})^\top \mathbf{t}_u^{(t)}}{\|\mathbf{t}_v^{(t)}\| \|\mathbf{t}_u^{(t)}\|}, \quad (4)$$

and the structural similarity

$$\text{sim}_s(v, u) = \frac{\mathbf{s}_v^\top \mathbf{s}_u}{\|\mathbf{s}_v\| \|\mathbf{s}_u\|}. \quad (5)$$

These two components are combined into a joint similarity score

$$S(v, u) = \alpha \text{sim}_t(v, u) + (1 - \alpha) \text{sim}_s(v, u), \quad (6)$$

where  $\alpha \in [0, 1]$  controls the trade-off between semantic and structural proximity. This design allows the retriever to adapt to different graph regimes, emphasizing textual semantics in text-rich graphs and structural roles in topology-dominated graphs.

For each target node  $v$ , all candidate nodes  $u \in \mathcal{V} \setminus \{v\}$  are ranked according to  $S(v, u)$ . From the top-ranked candidates, we further incorporate model confidence stored in the predictive state  $\mathbf{p}_u^{(t)}$  to filter unreliable references. Specifically, nodes with low predictive entropy or consistently correct predictions are preferred. The resulting exemplar set  $\mathcal{S}_v^{(t)}$  thus consists of in-graph references that are not only close to  $v$  in the joint semantic–structural space, but also stable with respect to the current task model.

Formally, for each target node  $v$ , we first rank all candidate nodes  $u \in \mathcal{V} \setminus \{v\}$  by the joint similarity score  $S(v, u)$ . Let  $\mathcal{C}_v^{(t)}$  denote the top- $K$  candidates under this ranking. We then define a confidence score for each candidate node  $u$  based on the predictive distribution  $\mathbf{p}_u^{(t)}$ , for example using the normalized entropy

$$H(u) = - \sum_{c \in \mathcal{Y}} p_u^{(t)}(c) \log p_u^{(t)}(c). \quad (7)$$

The final exemplar set is selected as

$$\mathcal{S}_v^{(t)} = \left\{ u \in \mathcal{C}_v^{(t)} \mid H(u) \leq \tau \right\}, \quad (8)$$

where  $\tau$  is a confidence threshold. This ensures that selected exemplars are both similar to  $v$  in the joint semantic–structural space and reliable under the current classifier.

## 2.5 Memory-Guided Semantic Refinement

Given the history memory  $\mathcal{B}^{(t)}$  at iteration  $t$ , DAS updates node semantics through a in-context refinement operator. This operator defines how the current description of each node is locally reshaped under task-aligned, in-graph references.

**Semantic Refinement Operator.** For each node  $v \in \mathcal{V}$ , an exemplar set  $\mathcal{S}_v^{(t)} \subset \mathcal{B}^{(t)}$  is first retrieved based on joint semantic–structural similarity and model stability. The large language model  $\mathcal{M}$  is then applied as a conditional refinement operator  $d_v^{(t+1)} = \mathcal{M}(d_v^{(t)}, \mathcal{S}_v^{(t)})$ , where  $d_v^{(t+1)}$  denotes the refined semantic description at iteration  $t + 1$ .

The LLM is instructed to perform *semantic reweighting and compression* rather than knowledge expansion. Specifically, it reconstructs  $d_v^{(t)}$  by emphasizing discriminative cues implicitly indicated by the exemplar set  $\mathcal{S}_v^{(t)}$ , while remaining faithful to the existing content. Since  $\mathcal{S}_v^{(t)}$  is drawn from the same graph and filtered by the current classifier, the refinement is implicitly shaped by both structural context and task supervision.

**Parallel Update.** The refinement in Eq. (10) is applied to all nodes in parallel, yielding

$$\mathcal{D}^{(t+1)} = \{d_v^{(t+1)} \mid v \in \mathcal{V}\}. \quad (9)$$

These updated descriptions are re-encoded as node features for the next training stage of the fixed GNN, which in turn updates the predictive state used to construct the next memory  $\mathcal{B}^{(t+1)}$ .

**Iterative Semantic Evolution.** Starting from the initialization  $d_v^{(0)} = r_v$ , the refinement proceeds as

$$d_v^{(0)} \rightarrow d_v^{(1)} \rightarrow \dots \rightarrow d_v^{(T)}. \quad (10)$$

Early iterations primarily reflect coarse lexical and structural cues, while later iterations progressively concentrate on task-discriminative semantics shaped by model feedback. After  $T$  iterations, the final descriptions  $\{d_v^{(T)}\}$  are used for evaluation.

## 2.6 Why Iterative Refinement Works

To further explain why DAS benefits from iterative semantic refinement, we provide a theoretical analysis in Appendix B. Specifically, we formalize DAS

	Nodes	Edges	Classes	Graph Types
Cora	2,708	10,556	7	Text-attribute
Pubmed	19,717	88,648	3	Text-attribute
USA	1,190	28,388	4	Text-free
Europe	399	12,385	4	Text-free
Brazil	131	2,137	4	Text-free

Table 1: Dataset statistics used in our experiments.

as an alternating optimization process over model parameters and node semantics, where the model-conditioned memory induces a task-adaptive surrogate objective. We show that, under mild assumptions, each refinement iteration is guaranteed not to increase this global objective. This result explains why DAS can progressively improve node semantics without suffering from uncontrolled semantic drift, and clarifies that the refinement loop constitutes a principled optimization process rather than heuristic text rewriting.

## 3 Experiments

### 3.1 Experimental Setup

**Datasets.** We evaluate on five graphs following Wang et al. (2025a): two text-attributed citation networks, Cora and Pubmed, and three text-free airport networks, USA, Europe, and Brazil (Statistics are given in Table 1). For Cora/Pubmed, nodes are papers (title+abstract), edges are citations, and classes are research topics. For airports, nodes are airports, edges are flight connections, and classes correspond to activity levels (Ribeiro et al., 2017).

**Baselines.** For text-attributed graphs, we compare Raw Feat. (bag-of-words/TF-IDF), Raw Text (use original text), TAPE (He et al., 2024), KEA (Chen et al., 2024b), and TANS (Wang et al., 2025a). For text-free graphs, we compare hand-crafted topology features—Node Degree, Eigenvector (Dwivedi et al., 2023), Random Walk (Dwivedi et al., 2022), and TANS (Wang et al., 2025a). In all text-attributed baselines, generated texts are appended to the original node text and encoded by the same sentence encoder for fairness, while for text-free graphs, the generated texts are used directly as node descriptions.

**Evaluation Protocol.** Unless otherwise specified, we focus on node classification with a GCN backbone (Kipf and Welling, 2017). We also report results with GAT (Veličković et al., 2018) and MLP in the text-attributed setting, following Wang et al. (2025a). For single-graph learning, we adopt

Method	Low-Label			High-Label			A.R.	
	GCN	GAT	MLP	GCN	GAT	MLP		
Cora	Raw Feat.	78.39 ± 1.69	79.31 ± 1.70	66.18 ± 4.95	83.10 ± 1.69	82.45 ± 1.23	64.56 ± 1.95	6.00
	Raw Text	79.19 ± 1.63	80.09 ± 1.57	70.55 ± 1.40	87.45 ± 1.15	85.72 ± 1.47	78.95 ± 1.45	4.83
	+ TAPE	79.64 ± 1.36	80.28 ± 1.37	70.97 ± 2.02	87.69 ± 1.34	86.21 ± 1.33	80.07 ± 1.72	3.50
	+ KEA	80.08 ± 1.71	79.80 ± 1.58	70.72 ± 1.51	87.94 ± 1.28	86.58 ± 1.10	79.90 ± 1.83	3.67
	+ TANS	80.66 ± 1.77	81.08 ± 1.62	72.47 ± 1.96	89.17 ± 1.17	88.23 ± 1.26	81.44 ± 1.42	2.00
	+ DAS (Ours)	<b>80.81 ± 1.39</b>	<b>81.43 ± 2.20</b>	<b>72.89 ± 2.21</b>	<b>89.31 ± 1.14</b>	<b>88.78 ± 1.17</b>	<b>81.87 ± 1.67</b>	<b>1.00</b>
Pubmed	Raw Feat.	75.39 ± 1.51	74.59 ± 1.36	68.01 ± 1.99	84.10 ± 0.55	84.31 ± 0.66	80.56 ± 0.30	6.00
	Raw Text	76.97 ± 1.95	75.50 ± 2.03	70.78 ± 2.00	87.49 ± 0.54	87.20 ± 0.51	82.58 ± 0.38	4.17
	+ TAPE	76.50 ± 3.27	75.30 ± 1.92	71.06 ± 2.13	88.21 ± 0.62	87.80 ± 0.48	83.98 ± 0.59	3.67
	+ KEA	<b>76.88 ± 1.73</b>	75.74 ± 2.06	71.32 ± 2.51	88.10 ± 0.49	87.77 ± 0.50	85.33 ± 0.41	3.17
	+ TANS	76.27 ± 2.35	76.99 ± 2.02	73.64 ± 2.59	89.17 ± 1.17	87.98 ± 0.48	88.84 ± 0.43	2.50
	+ DAS (Ours)	76.49 ± 2.57	<b>77.71 ± 3.19</b>	<b>74.30 ± 2.39</b>	<b>89.87 ± 0.55</b>	<b>88.57 ± 0.64</b>	<b>88.95 ± 0.79</b>	<b>1.50</b>

Table 2: Experimental results on text-attributed graphs. Boldface indicates the best and A.R. is the average ranking.

Method	Low-Label			High-Label			A.R.
	Europe	USA	Brazil	Europe	USA	Brazil	
Raw Feat. (One-Hot)	51.89 ± 2.75	52.74 ± 2.25	65.15 ± 15.93	54.61 ± 5.91	60.88 ± 3.83	49.88 ± 11.50	5.83
Node Degree	54.69 ± 3.35	59.93 ± 2.21	<b>71.82 ± 12.28</b>	55.72 ± 5.12	64.36 ± 3.18	63.83 ± 9.35	3.50
Eigenvector	55.80 ± 2.47	57.72 ± 2.19	62.42 ± 13.83	58.15 ± 4.51	63.66 ± 2.88	65.06 ± 8.95	3.83
Random Walk	56.70 ± 2.47	56.11 ± 2.11	69.70 ± 14.34	55.71 ± 4.01	62.80 ± 3.01	68.40 ± 9.65	3.67
TANS	55.56 ± 1.52	<b>61.08 ± 2.71</b>	65.73 ± 11.91	56.33 ± 5.73	65.81 ± 3.11	71.60 ± 10.66	2.67
DAS (Ours)	<b>56.80 ± 2.79</b>	60.01 ± 2.19	69.09 ± 10.65	<b>59.38 ± 5.05</b>	<b>67.23 ± 3.41</b>	<b>75.19 ± 7.42</b>	<b>1.50</b>

Table 3: Experimental results on text-free graphs with GCN as backbone.

the low-label / high-label splits: in the low-label regime, we use 20/30 nodes per class for train/valid on Cora/Pubmed (10/20 for Brazil); in the high-label regime, we use a 60/20/20 train/valid/test split. All reported numbers are averages over 30 random seeds with mean ± standard deviation, selecting models by the best validation accuracy. For the text encoder, we adopt MiniLM (Wang et al., 2020) unless otherwise noted.

### 3.2 Results on Text-Attributed Graphs

Table 2 reports node classification accuracy on text-attributed Cora and Pubmed under both low- and high-label settings, using GCN, GAT, and MLP backbones. On both of these datasets, augmenting Raw Text with existing LLM-based methods consistently improves performance over Raw Feat. and Raw Text across all backbones in both label regimes. Our method further improves upon the other methods in all configurations, consistently getting an accuracy higher than TANS for all backbones. These results indicate that structure-aware refinement is robust across architectures and scales of text-attributed citation graphs.

### 3.3 Results on Text-Free Graphs

We evaluate DAS on three text-free airport graphs using GCN as the backbone. Table 3 reports results under both low- and high-label splits. In the low-label regime, structural baselines such as Node Degree, Eigenvector, and Random Walk outperform

the one-hot feature baseline, confirming the importance of topology. DAS matches or surpasses these baselines on all three graphs, achieving the best accuracy on Europe and comparable performance on USA and Brazil. In the high-label regime, DAS yields clearer gains, achieving the strongest performance on USA and Brazil, and also outperforming all baselines on Europe. Notably, although no human-written text is available, DAS leverages structural cues to retrieve exemplars and progressively induces task-aligned node semantics through refinement. This structure-guided semantic evolution likely explains why gains on text-free graphs are larger than on text-attributed citation networks, where strong node texts already exist. Overall, these results indicate that iterative, structure-aware refinement is particularly effective when raw node features are absent and structural roles dominate.

### 3.4 Results under Distribution Shift

We assess cross-graph generalization in domain adaptation, where the model is trained on a source graph and directly evaluated on a target graph without fine-tuning. We train on a source graph and evaluate on a target graph (20% val / 80% test on target). We adopt the source→target pairs from Wang et al. (2025a) on the three airport graphs. Results in Table 4 show that TANS already improves over SVD-based alignment and purely structural features in most transfer directions. Our method

Source → Target →	USA		Europe		Brazil		A.R.
	Europe	Brazil	USA	Brazil	USA	Europe	
Raw Feat. (One-Hot) + SVD	–	–	–	–	–	–	–
Node Degree	30.55 ± 4.61	34.23 ± 5.19	45.90 ± 3.90	57.21 ± 5.30	24.95 ± 3.19	45.48 ± 2.58	5.00
Eigenvector	46.61 ± 1.54	52.29 ± 3.91	<b>53.40 ± 1.09</b>	66.76 ± 3.85	54.35 ± 2.22	51.85 ± 2.14	2.17
Random Walk	37.73 ± 3.08	32.79 ± 4.49	50.12 ± 1.76	61.49 ± 4.33	25.43 ± 0.98	50.96 ± 4.42	5.00
TANS	48.79 ± 2.60	58.13 ± 3.38	49.45 ± 1.59	62.38 ± 5.98	44.82 ± 1.65	52.71 ± 2.09	3.00
TANS	50.99 ± 3.31	67.17 ± 4.68	51.88 ± 2.82	71.59 ± 3.97	<b>54.96 ± 1.80</b>	53.79 ± 2.15	2.17
<b>DAS (Ours)</b>	<b>51.96 ± 3.04</b>	<b>68.78 ± 12.80</b>	51.91 ± 2.95	<b>73.33 ± 5.55</b>	53.78 ± 3.44	<b>54.47 ± 2.18</b>	<b>1.67</b>

Table 4: Experimental results on domain adaptation setting.

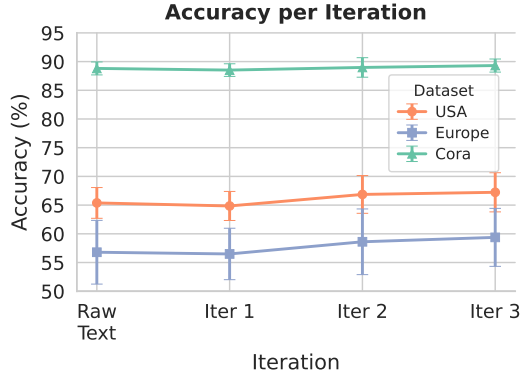


Figure 3: The impact of the number of iterations.

further increases accuracy in the majority of source-target pairs. For example, when transferring from USA to Europe or Brazil, and from Europe to Brazil, we achieve the best performance among all methods. The performance gains of our method are especially notable on more challenging transfers involving Brazil, where structural roles differ markedly across graphs. These improvements suggest that iteratively refined, structure-aware node texts provide a more transferable representation than synthesized descriptions.

#### 4 Mechanism Analysis

This section analyzes the key mechanisms underlying DAS beyond aggregate performance. We focus on how iterative refinement and history-guided exemplar retrieval shape semantic evolution, and characterize when these mechanisms succeed or fail. We provide additional analysis in Appendix F

**The Role of Iterative Refinement.** We analyze whether iterative refinement is necessary beyond a single-round semantic update. We vary the number of refinement iterations  $T \in \{1, 2, 3\}$  on a text-attributed graph (Cora) and two text-free graphs (USA, Europe). Figure 3 reports the accuracy improvement over using raw node descriptions. Across all datasets, performance improves monotonically as  $T$  increases, indicating that semantic refinement benefits from repeated feedback

Setting	Cora	USA
DAS (Ours)	<b>89.31 ± 1.14</b>	<b>67.23 ± 3.41</b>
Structure-only	88.94 ± 1.07	66.29 ± 3.03
Text-only	89.09 ± 1.01	66.38 ± 2.80
Random exemplars	89.06 ± 0.92	66.47 ± 3.24

Table 5: Ablation results on memory.

rather than one-shot rewriting. This trend suggests that successive rounds allow the model-conditioned memory to accumulate more reliable exemplars, which in turn guide the LLM toward increasingly task-aligned descriptions. The marginal gain from  $T=2$  to  $T=3$  is small, indicating that a limited number of iterations suffices to realize most of the benefit, while keeping LLM cost manageable.

**The Role of Model-Conditioned Memory.** We examine the role of the model-conditioned memory in exemplar retrieval for semantic refinement. To isolate its effect, we compare DAS with three ablated variants: *Random* exemplar selection, *Structure-only* retrieval based solely on structural similarity, and *Text-only* retrieval based solely on semantic similarity. All variants use the same refinement procedure and prompt format.

Results in Table 5 show that joint semantic-structural retrieval in DAS consistently outperforms all ablated variants on both Cora and USA. On Cora, text-only retrieval performs competitively, reflecting the strong semantic signal in raw node texts, while structure-only retrieval is weaker. In contrast, on the text-free USA graph, both text-only and structure-only retrieval degrade performance, indicating that neither modality alone is sufficient for stable refinement. Random exemplar selection performs worst in both cases. These results demonstrate that effective refinement requires task-relevant exemplars that are aligned in both semantic content and structural role. The joint retrieval mechanism is particularly critical when node semantics must be induced from topology, where

relying on a single modality can introduce noisy or misleading in-context signals.

### **Why DAS Succeeds: Semantic Sharpening and Role Abstraction.**

DAS is most effective when iterative refinement sharpens task-discriminative evidence already latent in the input representations. On text-attributed graphs, successful refinement makes class-consistent technical cues more explicit, leading to reduced predictive entropy and corrections toward the true label. On text-free graphs, DAS succeeds when raw topological statistics are reorganized into a coherent semantic role interpretation (e.g., distinguishing regionally embedded nodes from global connectors based on clustering and betweenness). In both cases, refinement aligns node semantics more closely with the structure–semantics regime of the graph, enabling the classifier to make more confident and accurate predictions. Representative examples are provided in Table 7 in the appendix.

### **When DAS Fails: Drift and Over-Confidence.**

Failure cases reveal inherent limitations of LLM-based semantic refinement. One common failure mode is *label drift*, where rewrites improve fluency without introducing additional discriminative evidence, causing predictions to shift toward a semantically adjacent but incorrect class. Another failure mode is *over-confidence*, in which refinement reduces predictive entropy while the prediction itself remains incorrect. On text-free graphs, we additionally observe occasional *attribute drift*, where numeric structural attributes are subtly altered during rewriting, raising faithfulness concerns even when predictive accuracy improves. These failures highlight that effective refinement depends on maintaining a tight coupling between generated semantics and the underlying structural evidence. See Table 8 in the appendix for examples.

## **5 Related Work**

We provide a more detailed discussion of related work in Appendix A.

**GNNs and Fixed Inductive Bias.** Classical GNNs learn representations through local message passing, thereby encoding fixed inductive biases such as locality and homophily (Kipf and Welling, 2017; Hamilton et al., 2017; Veličković et al., 2018; Xu et al., 2019). Structure-only methods based on random walks or structural roles further impose predefined topological assumptions (Perozzi

et al., 2014; Grover and Leskovec, 2016; Ribeiro et al., 2017). While effective in specific regimes, these methods rely on fixed priors that do not adapt to heterogeneous structure–semantics distributions across graph domains.

**Model-Centric Refinement.** Most existing attempts to address structure–semantics heterogeneity remain *model-centric*. This includes strengthening GNN architectures with richer structural priors (Maron et al., 2018; Murphy et al., 2019; Jin et al., 2022), treating LLMs as direct graph reasoners via graph-to-text serialization (Zhao et al., 2023a; Kong et al., 2024; Chen et al., 2024a), and introducing auxiliary models to enrich node representations with external semantic signals (Yao et al., 2019; He et al., 2023; Yang et al., 2021). Despite their diversity, these approaches all inject additional inductive biases from the model side, and the construction of node representations remains largely static once the model is specified.

### **Data-Centric Refinement and Our Perspective.**

Existing data-centric methods primarily focus on graph augmentation, structure learning, or pseudo-labeling for robustness and generalization (You et al., 2020; Jin et al., 2020; Chen et al., 2023; He et al., 2023; Chen et al., 2024b), rather than on adapting node semantics to task-specific structure–semantics regimes. In contrast, our work treats node semantics as task-adaptive variables and proposes a feedback-driven framework for iterative, structure-aware semantic refinement, providing a fundamentally different data-centric perspective for handling structure–semantics heterogeneity.

## **6 Conclusion**

In this work, we proposed DAS, a data-centric framework for iterative, structure-aware node semantic refinement on graphs. By coupling a fixed GNN with a large language model through a model-conditioned history memory, DAS enables node semantics to be progressively adapted under joint structural context and task feedback. Experiments on both text-rich and text-free graphs show that DAS consistently improves over strong LLM-as-enhancer baselines in structure-dominated settings while remaining competitive in semantics-rich regimes. More broadly, this work highlights a new direction for graph learning, where input representations are treated as dynamic, task-adaptive states rather than static features.

## Limitations

Although DAS provides a flexible data-centric mechanism for adapting node semantics to varying graph regimes, several limitations remain. First, the approach incurs non-trivial computational overhead because each refinement round requires a separate LLM inference pass over all nodes. While our experiments suggest that a small number of refinement iterations suffice on medium-sized graphs, scaling DAS to very large graphs or to settings requiring repeated retraining would be challenging without further optimization or model compression strategies. To this end, we can modify its refinement process refining only uncertain or representative nodes, offering a potential path toward scalability on larger graphs. Second, the quality and faithfulness of refined descriptions depend on the underlying language model. Weaker LLMs may fail to preserve structural cues, and even strong LLMs can occasionally introduce factual inconsistencies. Although our prompts explicitly discourage hallucination and require strict adherence to the original information, semantic drift may still occur in some cases. Finally, our study focuses primarily on node classification. Whether the same refinement dynamics hold for tasks such as link prediction, clustering, or graph-level classification remains an open question and a promising area for future work.

## Ethical Considerations

This work relies on large language models to generate or refine textual node descriptions. As with any LLM-based system, the outputs may inherit or amplify biases present in the pretraining data. When DAS is applied to graphs whose nodes represent people or sensitive entities, refined descriptions could potentially introduce or reinforce demographic stereotypes, even when the graph structure itself does not encode such information. Care should therefore be taken when deploying the method in sensitive domains. DAS also requires repeated LLM calls during iterative refinement. Depending on the model and API used, this may entail substantial computational and environmental cost. Although our experiments rely on a small number of refinement rounds, practitioners should be mindful of the carbon footprint and financial cost associated with large-scale deployment. Finally, DAS modifies node-level textual descriptions during training. While these refined descriptions

are not intended for human consumption and are not used to produce new factual knowledge, they may nonetheless be misinterpreted as authoritative explanations of the underlying graph if presented without context. We therefore recommend that systems built on DAS avoid exposing refined descriptions directly to end users unless appropriate disclaimers are provided.

## References

- Runjin Chen, Tong Zhao, Ajay Jaiswal, Neil Shah, and Zhangyang Wang. 2024a. Llava: Large language and graph assistant. *arXiv preprint arXiv:2402.08170*.
- Zhengdao Chen, Lei Chen, Soledad Villar, and Joan Bruna. 2020. Can graph neural networks count substructures? In *NeurIPS*.
- Zhengdao Chen, Soledad Villar, Lei Chen, and Joan Bruna. 2019. On the equivalence between graph isomorphism testing and function approximation with gnns. *Advances in neural information processing systems*, 32.
- Zhikai Chen, Haitao Mao, Hang Li, Wei Jin, Hongzhi Wen, Xiaochi Wei, Shuaiqiang Wang, Dawei Yin, Wenqi Fan, Hui Liu, and 1 others. 2024b. Exploring the potential of large language models (llms) in learning on graphs. *ACM SIGKDD Explorations Newsletter*, 25(2):42–61.
- Zhikai Chen, Haitao Mao, Jingzhe Liu, Yu Song, Bingheng Li, Wei Jin, Bahare Fatemi, Anton Tsitsulin, Bryan Perozzi, Hui Liu, and 1 others. 2024c. Text-space graph foundation models: Comprehensive benchmarks and new insights. In *NeurIPS*.
- Zhikai Chen, Haitao Mao, Hongzhi Wen, Haoyu Han, Wei Jin, Haiyang Zhang, Hui Liu, and Jiliang Tang. 2023. Label-free node classification on graphs with large language models (llms). *arXiv preprint arXiv:2310.04668*.
- Vijay Prakash Dwivedi, Chaitanya K Joshi, Anh Tuan Luu, Thomas Laurent, Yoshua Bengio, and Xavier Bresson. 2023. Benchmarking graph neural networks. *JMLR*.
- Vijay Prakash Dwivedi, Anh Tuan Luu, Thomas Laurent, Yoshua Bengio, and Xavier Bresson. 2022. Graph neural networks with learnable structural and positional representations. In *ICLR*.
- Yujie Fan, Mingxuan Ju, Chuxu Zhang, and Yanfang Ye. 2022. Heterogeneous temporal graph neural network. In *Proceedings of the 2022 SIAM international conference on data mining (SDM)*, pages 657–665. SIAM.
- Yi Fang, Dongzhe Fan, Daochen Zha, and Qiaoyu Tan. 2024. Gaugllm: Improving graph contrastive learning for text-attributed graphs with large language models. *arXiv preprint arXiv:2406.11945*.

- Steven A Greenberg. 2009. How citation distortions create unfounded authority: analysis of a citation network. *Bmj*, 339.
- Aditya Grover and Jure Leskovec. 2016. node2vec: Scalable feature learning for networks. In *Proceedings of the 22nd ACM SIGKDD international conference on Knowledge discovery and data mining*, pages 855–864.
- Jiayan Guo, Lun Du, and Hengyu Liu. 2023. Gpt4graph: Can large language models understand graph structured data? an empirical evaluation and benchmarking. *arXiv*.
- Will Hamilton, Zhitao Ying, and Jure Leskovec. 2017. Inductive representation learning on large graphs. In *NeurIPS*.
- Xiaolong Han, Yu Xue, Zehong Wang, Yong Zhang, Anton Muravev, and Moncef Gabbouj. 2024. Sadenas: A self-adaptive differential evolution algorithm for neural architecture search. *Swarm and Evolutionary Computation*, 91:101736.
- Xiaoxin He, Xavier Bresson, Thomas Laurent, Adam Perold, Yann LeCun, and Bryan Hooi. 2023. Harnessing explanations: Llm-to-lm interpreter for enhanced text-attributed graph representation learning. *arXiv preprint arXiv:2305.19523*.
- Xiaoxin He, Xavier Bresson, Thomas Laurent, Adam Perold, Yann LeCun, and Bryan Hooi. 2024. Harnessing explanations: LLM-to-LM interpreter for enhanced text-attributed graph representation learning. In *ICLR*.
- Di Jin, Rui Wang, Meng Ge, Dongxiao He, Xiang Li, Wei Lin, and Weixiong Zhang. 2022. Raw-gnn: Random walk aggregation based graph neural network. *arXiv preprint arXiv:2206.13953*.
- Wei Jin, Yao Ma, Xiaorui Liu, Xianfeng Tang, Suhang Wang, and Jiliang Tang. 2020. Graph structure learning for robust graph neural networks. In *Proceedings of the 26th ACM SIGKDD international conference on knowledge discovery & data mining*, pages 66–74.
- Thomas N. Kipf and Max Welling. 2017. Semi-supervised classification with graph convolutional networks. In *ICLR*.
- Lecheng Kong, Jiarui Feng, Hao Liu, Chengsong Huang, Jiaxin Huang, Yixin Chen, and Muhan Zhang. 2024. Gofa: A generative one-for-all model for joint graph language modeling. *arXiv preprint arXiv:2407.09709*.
- Yixin Liu, Yu Zheng, Daokun Zhang, Hongxu Chen, Hao Peng, and Shirui Pan. 2022. Towards unsupervised deep graph structure learning. In *Proceedings of the ACM Web Conference 2022*, pages 1392–1403.
- Andreas Loukas. 2019. What graph neural networks cannot learn: depth vs width. *arXiv preprint arXiv:1907.03199*.
- Sitao Luan, Chenqing Hua, Qincheng Lu, Jiaqi Zhu, Mingde Zhao, Shuyuan Zhang, Xiao-Wen Chang, and Doina Precup. 2022. Revisiting heterophily for graph neural networks. In *NeurIPS*.
- Haggai Maron, Heli Ben-Hamu, Hadar Serviansky, and Yaron Lipman. 2019. Provably powerful graph networks. *Advances in neural information processing systems*, 32.
- Haggai Maron, Heli Ben-Hamu, Nadav Shamir, and Yaron Lipman. 2018. Invariant and equivariant graph networks. *arXiv preprint arXiv:1812.09902*.
- Christopher Morris, Martin Ritzert, Matthias Fey, William L Hamilton, Jan Eric Lenssen, Gaurav Rattan, and Martin Grohe. 2019. Weisfeiler and leman go neural: Higher-order graph neural networks. In *AAAI*.
- Ryan Murphy, Balasubramaniam Srinivasan, Vinayak Rao, and Bruno Ribeiro. 2019. Relational pooling for graph representations. In *International Conference on Machine Learning*, pages 4663–4673. PMLR.
- Bryan Perozzi, Rami Al-Rfou, and Steven Skiena. 2014. Deepwalk: Online learning of social representations. In *Proceedings of the 20th ACM SIGKDD international conference on Knowledge discovery and data mining*, pages 701–710.
- Bryan Perozzi, Bahare Fatemi, Dustin Zelle, Anton Tsitsulin, Mehran Kazemi, Rami Al-Rfou, and Jonathan Halcrow. 2024. Let your graph do the talking: Encoding structured data for llms. *arXiv preprint arXiv:2402.05862*.
- Oleg Platonov, Denis Kuznedelev, Artem Babenko, and Liudmila Prokhorenkova. 2023. Characterizing graph datasets for node classification: Homophily-heterophily dichotomy and beyond. *Advances in Neural Information Processing Systems*, 36:523–548.
- Ladislav Rampásek, Michael Galkin, Vijay Prakash Dwivedi, Anh Tuan Luu, Guy Wolf, and Dominique Beaini. 2022. Recipe for a general, powerful, scalable graph transformer. *Advances in Neural Information Processing Systems*, 35:14501–14515.
- Leonardo FR Ribeiro, Pedro HP Saverese, and Daniel R Figueiredo. 2017. struc2vec: Learning node representations from structural identity. In *KDD*.
- Jari Saramäki, Mikko Kivelä, Jukka-Pekka Onnela, Kimmo Kaski, and Janos Kertesz. 2007. Generalizations of the clustering coefficient to weighted complex networks. *Physical Review E—Statistical, Nonlinear, and Soft Matter Physics*.
- Ying Sun, Prabhu Babu, and Daniel P Palomar. 2016. Majorization-minimization algorithms in signal processing, communications, and machine learning. *IEEE Transactions on Signal Processing*, 65(3):794–816.

- Susheel Suresh, Pan Li, Cong Hao, and Jennifer Neville. 2021. Adversarial graph augmentation to improve graph contrastive learning. *Advances in Neural Information Processing Systems*, 34:15920–15933.
- Jan Tönshoff, Martin Ritzert, Hinrikus Wolf, and Martin Grohe. 2021. Walking out of the weisfeiler leman hierarchy: Graph learning beyond message passing. *arXiv preprint arXiv:2102.08786*.
- Petar Veličković, Guillem Cucurull, Arantxa Casanova, Adriana Romero, Pietro Liò, and Yoshua Bengio. 2018. Graph attention networks. In *ICLR*.
- Heng Wang, Shangbin Feng, Tianxing He, Zhaoxuan Tan, Xiaochuang Han, and Yulia Tsvetkov. 2023a. Can language models solve graph problems in natural language? *Advances in Neural Information Processing Systems*, 36:30840–30861.
- Wenhui Wang, Furu Wei, Li Dong, Hangbo Bao, Nan Yang, and Ming Zhou. 2020. Minilm: Deep self-attention distillation for task-agnostic compression of pre-trained transformers. In *NeurIPS*.
- Zehong Wang, Qi Li, Donghua Yu, Xiaolong Han, Xiao-Zhi Gao, and Shigen Shen. 2023b. Heterogeneous graph contrastive multi-view learning. In *Proceedings of the 2023 SIAM international conference on data mining (SDM)*, pages 136–144. SIAM.
- Zehong Wang, Sidney Liu, Zheyuan Zhang, Tianyi Ma, Chuxu Zhang, and Yanfang Ye. 2025a. Can llms convert graphs to text-attributed graphs? In *Proceedings of the 2025 Conference of the Nations of the Americas Chapter of the Association for Computational Linguistics: Human Language Technologies (Volume 1: Long Papers)*, pages 1412–1432.
- Zehong Wang, Donghua Yu, Shigen Shen, Shichao Zhang, Huawen Liu, Shuang Yao, and Maozu Guo. 2024a. Select your own counterparts: Self-supervised graph contrastive learning with positive sampling. *IEEE Transactions on Neural Networks and Learning Systems*, 36(4):6858–6872.
- Zehong Wang, Zheyuan Zhang, Nitesh V Chawla, Chuxu Zhang, and Yanfang Ye. 2024b. Gft: Graph foundation model with transferable tree vocabulary. In *NeurIPS*.
- Zehong Wang, Zheyuan Zhang, Tianyi Ma, Nitesh V Chawla, Chuxu Zhang, and Yanfang Ye. 2025b. Beyond message passing: Neural graph pattern machine. In *Forty-second International Conference on Machine Learning*.
- Zehong Wang, Zheyuan Zhang, Tianyi Ma, Nitesh V Chawla, Chuxu Zhang, and Yanfang Ye. 2025c. Towards graph foundation models: Learning generalities across graphs via task-trees. In *Forty-second International Conference on Machine Learning*.
- Zehong Wang, Zheyuan Zhang, Tianyi Ma, Chuxu Zhang, and Yanfang Ye. 2025d. Generative graph pattern machine. In *The Thirty-ninth Annual Conference on Neural Information Processing Systems*.
- Zhihao Wen and Yuan Fang. 2023. Augmenting low-resource text classification with graph-grounded pre-training and prompting. In *Proceedings of the 46th International ACM SIGIR Conference on Research and Development in Information Retrieval*, pages 506–516.
- Zhenqin Wu, Bharath Ramsundar, Evan N Feinberg, Joseph Gomes, Caleb Geniesse, Aneesh S Pappu, Karl Leswing, and Vijay Pande. 2018. Moleculenet: a benchmark for molecular machine learning. *Chemical science*, 9(2):513–530.
- Zonghan Wu, Shirui Pan, Fengwen Chen, Guodong Long, Chengqi Zhang, and S Yu Philip. 2020. A comprehensive survey on graph neural networks. *TNNLS*.
- Keyulu Xu, Weihua Hu, Jure Leskovec, and Stefanie Jegelka. 2019. How powerful are graph neural networks? In *ICLR*.
- Yu Xue, Xiaolong Han, and Zehong Wang. 2024. Self-adaptive weight based on dual-attention for differentiable neural architecture search. *IEEE Transactions on Industrial Informatics*, 20(4):6394–6403.
- Hao Yan, Chaozhuo Li, Ruosong Long, Chao Yan, Jianan Zhao, Wenwen Zhuang, Jun Yin, Peiyan Zhang, Weihao Han, Hao Sun, and 1 others. 2023. A comprehensive study on text-attributed graphs: Benchmarking and rethinking. *Advances in Neural Information Processing Systems*, 36:17238–17264.
- Haoran Yang, Qian Liu, Dechuan Zeng, Fuzhen Zhang, and Wenjie Li. 2024. Latex-gcl: Large language models (llms)-based data augmentation for text-attributed graph contrastive learning. *arXiv preprint arXiv:2409.01145*.
- Junhan Yang, Zheng Liu, Shitao Xiao, Chaozhuo Li, Defu Lian, Sanjay Agrawal, Amit Singh, Guangzhong Sun, and Xing Xie. 2021. Graphformers: Gnn-nested transformers for representation learning on textual graph. *Advances in Neural Information Processing Systems*, 34:28798–28810.
- Liang Yao, Chengsheng Mao, and Yuan Luo. 2019. Graph convolutional networks for text classification. In *Proceedings of the AAAI conference on artificial intelligence*, volume 33, pages 7370–7377.
- Yanfang Ye, Zheyuan Zhang, Tianyi Ma, Zehong Wang, Yiyang Li, Shifu Hou, Weixiang Sun, Kaiwen Shi, Yijun Ma, Wei Song, and 1 others. 2025. Llms4all: A systematic review of large language models across academic disciplines. *arXiv preprint arXiv:2509.19580*.
- Zhitao Ying, Jiaxuan You, Christopher Morris, Xiang Ren, Will Hamilton, and Jure Leskovec. 2018. Hierarchical graph representation learning with differentiable pooling. *Advances in neural information processing systems*, 31.

- Yuning You, Tianlong Chen, Yang Shen, and Zhangyang Wang. 2021. Graph contrastive learning automated. In *International conference on machine learning*, pages 12121–12132. PMLR.
- Yuning You, Tianlong Chen, Yongduo Sui, Ting Chen, Zhangyang Wang, and Yang Shen. 2020. Graph contrastive learning with augmentations. *Advances in neural information processing systems*, 33:5812–5823.
- Bohang Zhang, Jingchu Gai, Yiheng Du, Qiwei Ye, Di He, and Liwei Wang. 2024a. Beyond weisfeiler-lehman: A quantitative framework for gnn expressiveness. In *ICLR*.
- Chuxu Zhang, Dongjin Song, Chao Huang, Ananthram Swami, and Nitesh V Chawla. 2019a. Heterogeneous graph neural network. In *Proceedings of the 25th ACM SIGKDD international conference on knowledge discovery & data mining*, pages 793–803.
- Chuxu Zhang, Ananthram Swami, and Nitesh V Chawla. 2019b. Shne: Representation learning for semantic-associated heterogeneous networks. In *Proceedings of the twelfth ACM international conference on web search and data mining*, pages 690–698.
- Delvin Ce Zhang, Menglin Yang, Rex Ying, and Hady W Lauw. 2024b. Text-attributed graph representation learning: Methods, applications, and challenges. In *Companion Proceedings of the ACM Web Conference 2024*, pages 1298–1301.
- Junlong Zhang and Yu Luo. 2017. Degree centrality, betweenness centrality, and closeness centrality in social network. In *MSAM2017*.
- Peng Zhang, Jinliang Wang, Xiaojia Li, Menghui Li, Zengru Di, and Ying Fan. 2008. Clustering coefficient and community structure of bipartite networks. *Physica A: Statistical Mechanics and its Applications*.
- Zheyuan Zhang, Zehong Wang, Tianyi Ma, Varun Sameer Taneja, Sofia Nelson, Nhi Ha Lan Le, Keerthiram Murugesan, Mingxuan Ju, Nitesh V Chawla, Chuxu Zhang, and 1 others. 2025. Mopihfrs: A multi-objective personalized health-aware food recommendation system with llm-enhanced interpretation. In *Proceedings of the 31st ACM SIGKDD Conference on Knowledge Discovery and Data Mining V. 1*, pages 2860–2871.
- Ziwei Zhang, Peng Cui, and Wenwu Zhu. 2020. Deep learning on graphs: A survey. *IEEE Transactions on Knowledge and Data Engineering*, 34(1):249–270.
- Dangzhi Zhao and Andreas Strotmann. 2015. *Analysis and visualization of citation networks*. Morgan & Claypool Publishers.
- Jianan Zhao, Meng Qu, Chaozhuo Li, Hao Yan, Qian Liu, Rui Li, Xing Xie, and Jian Tang. 2022. Learning on large-scale text-attributed graphs via variational inference. *arXiv preprint arXiv:2210.14709*.
- Jianan Zhao, Xiao Wang, Chuan Shi, Binbin Hu, Guojie Song, and Yanfang Ye. 2021a. Heterogeneous graph structure learning for graph neural networks. In *Proceedings of the AAAI conference on artificial intelligence*, volume 35, pages 4697–4705.
- Jianan Zhao, Le Zhuo, Yikang Shen, Meng Qu, Kai Liu, Michael Bronstein, Zhaocheng Zhu, and Jian Tang. 2023a. Graphtext: Graph reasoning in text space. *arXiv preprint arXiv:2310.01089*.
- Tong Zhao, Yozen Liu, Leonardo Neves, Oliver Woodford, Meng Jiang, and Neil Shah. 2021b. Data augmentation for graph neural networks. In *Proceedings of the aaai conference on artificial intelligence*, volume 35, pages 11015–11023.
- Wayne Xin Zhao, Kun Zhou, Junyi Li, Tianyi Tang, Xiaolei Wang, Yupeng Hou, Yingqian Min, Beichen Zhang, Junjie Zhang, Zican Dong, and 1 others. 2023b. A survey of large language models. *arXiv*.
- Yanqiao Zhu, Yichen Xu, Feng Yu, Qiang Liu, Shu Wu, and Liang Wang. 2021. Graph contrastive learning with adaptive augmentation. In *Proceedings of the web conference 2021*, pages 2069–2080.

## A Comprehensive Related Work

### A.1 GNNs with Fixed Inductive Bias

Classical graph representation learning is largely built upon fixed inductive biases that encode how structural and semantic information is propagated and aggregated over the graph. Early message-passing GNNs (Kipf and Welling, 2017; Hamilton et al., 2017; Veličković et al., 2018) propagate input node features through local neighborhood aggregation to learn task-specific representations. By design, these architectures favor locality and homophily (Xu et al., 2019; Luan et al., 2022), thereby imposing a strong but fixed prior on how predictive signals are assumed to distribute over the graph. Complementary to message-passing models, structure-only methods characterize nodes by their positional or role similarity using random walks and structural homophily. Representative approaches include DeepWalk (Perozzi et al., 2014), node2vec (Grover and Leskovec, 2016), and struc2vec (Ribeiro et al., 2017), which learn embeddings purely from graph topology without relying on node semantics. While highly effective in structure-dominated settings, these methods likewise rely on pre-specified structural assumptions that remain fixed across graph domains. Motivated by this limitation, a large body of subsequent work has sought to address structure–semantics mismatch primarily from the model side, by designing new architectures and learning mechanisms with enhanced inductive biases.

### A.2 Model-Centric Adaptation

**Advanced GNN Model Architecture.** A prominent line of model-centric approaches seeks to address structure–semantics heterogeneity by directly strengthening the inductive bias of GNN architectures (Xue et al., 2024; Han et al., 2024). These methods go beyond standard message passing by encoding richer structural priors into the model design. For instance, Maron et al. (2018); Chen et al. (2019); Maron et al. (2019) propose  $k$ -order Weisfeiler–Lehman (WL) GNNs to emulate the  $k$ -WL test within neural architectures, while Murphy et al. (2019); Loukas (2019) introduce positional and relational encodings to enhance representational power. Another line of work leverages random walk kernels to guide the message passing process, further enriching the inductive bias of existing GNNs (Jin et al., 2022; Tönshoff et al., 2021; Wang et al., 2025b,d). Despite improved

expressivity, these models remain fundamentally model-centric: the inductive biases are still explicitly predefined by architecture design. Moreover, many remain theoretically bounded by the  $k$ -WL hierarchy (Zhang et al., 2024a), suggesting that architectural enhancement alone cannot offer a principled solution to the open-ended diversity of real-world graphs.

**LLMs as Reasoners.** Another emerging model-centric paradigm treats LLMs as direct graph reasoners. These methods linearize graph structures and node attributes into natural language prompts and rely on the general reasoning capabilities of LLMs for training-free or lightly supervised graph classification and question answering (Zhao et al., 2023a; Guo et al., 2023; Wang et al., 2023a; Kong et al., 2024; Chen et al., 2024a). For example, Wang et al. (2023a) describes graphs in natural language and applies LLMs to solve basic graph reasoning tasks, while GOFA (Kong et al., 2024) and LLaGA (Chen et al., 2024a) operate over serialized graph representations or graph embeddings for downstream inference. By bypassing explicit message passing, these approaches effectively replace graph-specific inductive biases with the intrinsic reasoning priors of LLMs. However, this paradigm remains model-centric: structural information is processed solely according to the LLM and the serialization scheme, and context length limits together with the loss of explicit topology constrain scalability and long-range structural modeling.

### Auxiliary Models to Enhance Graph Models.

Beyond architectural modification and language-based reasoning, another class of model-centric approaches introduces auxiliary models to enrich the input representations of graph learners. Early work such as TextGCN (Yao et al., 2019) demonstrates the benefit of incorporating external textual semantics into graph learning. More recently, with the advent of LLMs, a growing body of methods leverage LLMs as semantic enhancers to generate or refine node descriptions for downstream GNNs (Chen et al., 2024c; Zhang et al., 2024b; Yan et al., 2023; He et al., 2023; Chen et al., 2024b; Wang et al., 2025a; Yang et al., 2024; Fang et al., 2024). In parallel, some works align auxiliary models with GNNs via joint training or embedding alignment (Yang et al., 2021; Zhao et al., 2022; Wen and Fang, 2023). Despite their effectiveness, these approaches remain model-centric: auxiliary models inject additional semantic or structural inductive

biases, while the resulting node representations are typically treated as static inputs by the downstream GNN rather than being refined under task-driven feedback.

**Limitations of Model-Centric Methods.** Despite their empirical success, the above paradigms share a fundamental commonality: they all address structure–semantics heterogeneity by injecting additional inductive biases from the model side. Whether through architectural design, language-based reasoning, or auxiliary semantic enhancement, the manner in which semantic and structural information is combined is still determined by pre-specified model mechanisms. However, real-world graph distributions are open-ended and structurally diverse, making it fundamentally impossible for any finite collection of model-level biases to guarantee universal adaptability. Moreover, most model-centric approaches construct node representations in a largely static manner with respect to downstream learning dynamics, limiting their ability to adapt data representations to graph-specific structure–semantics regimes.

### A.3 Data-Centric Adaptation

Beyond modifying graph learning models, another line of research adopts a data-centric perspective by directly manipulating the graph data or input representations. Most existing data-centric approaches are developed primarily for representation robustness, regularization, or generalization, rather than for explicitly addressing structure–semantics heterogeneity.

**Graph Data Augmentation.** A large body of work focuses on graph data augmentation, where node features or graph structures are perturbed to construct multiple views of the same graph for invariant representation learning (Zhao et al., 2021b; Zhu et al., 2021; Suresh et al., 2021; You et al., 2020, 2021; Wang et al., 2023b, 2024a). For example, GraphCL (You et al., 2020) applies a set of predefined structural and feature augmentations to generate contrastive graph views, enabling a model to capture augmentation-invariant information. These methods are effective for improving robustness and transferability, but the underlying node semantics are not explicitly refined toward task-specific semantic–structural alignment.

**Graph Structure Learning.** Another line of data-centric work focuses on graph structure learn-

ing, which aims to optimize or reconstruct graph connectivity to better support GNN training (Jin et al., 2020; Liu et al., 2022; Zhao et al., 2021a; Zhang et al., 2025; Perozzi et al., 2024). These approaches adapt the graph topology by removing spurious edges or adding task-relevant connections, thereby modifying the structural substrate on which message passing operates. However, they primarily operate at the level of graph structure and do not directly model how node semantics should be adapted under different structure–semantics regimes.

**Pseudo-Labeling.** In addition, several studies explore pseudo-labeling and self-training schemes to guide representation learning in low-label settings (Chen et al., 2023). While effective for label efficiency, such methods treat node features as fixed inputs and do not address the problem of task-driven semantic adaptation under structural context.

**The Position of Our Work.** In contrast to the above data-centric paradigms, our work targets a fundamentally different objective. Rather than augmenting data for invariance, modifying graph structure, or propagating pseudo-label supervision, we focus on *task-driven refinement of node semantics themselves*. Our method treats node semantics as *adaptive variables* that are progressively reshaped under structural context and predictive feedback from a downstream GNN, enabling direct handling of structure–semantics heterogeneity at the level where the balance between structure and semantics is instantiated.

## B Understanding DAS: Why Iterative Semantic Refinement Works

We provide a theoretical interpretation of DAS as a generalized *Majorization–Minimization* (MM) procedure (Sun et al., 2016). We show that the iterative refinement loop monotonically decreases a task-adaptive surrogate objective, where the model-conditioned memory induces a tractable majorizer for semantic refinement.

### B.1 Problem Formulation

Let  $\mathcal{D} = \{d_v\}_{v \in \mathcal{V}}$  be the set of node descriptions and let  $\mathbf{t}(d_v)$  denote the sentence embedding of  $d_v$ . We define the global objective as

$$\mathcal{J}(\theta, \mathcal{D}) = \sum_{v \in \mathcal{V}_{\text{train}}} \ell(y_v, g_\theta(\mathbf{x}(d_v), G)) + \lambda \mathcal{R}(\mathcal{D}), \quad (11)$$

where  $\ell$  is the supervised loss and  $\mathcal{R}$  is a memory-consistency regularizer defined below.

**Implicit Memory-Consistency Regularizer.** At iteration  $t$ , DAS retrieves an exemplar set  $\mathcal{S}_v^{(t)}$  from the model-conditioned memory  $\mathcal{B}^{(t)}$ . Given a candidate description set  $\mathcal{D}$ , consider the following admissible anchor set for each node:

$$\mathcal{M}_v(\mathcal{D}) = \left\{ \frac{1}{|\mathcal{S}_v|} \sum_{u \in \mathcal{S}_v} \mathbf{t}(d_u) \right\}, \quad (12)$$

where  $C : \mathcal{S}_v \subseteq \mathcal{V} \setminus \{v\}$ ,  $|\mathcal{S}_v| \leq K$ .

i.e., anchors induced by averaging embeddings of up to  $K$  in-graph exemplars. In practice,  $\mathcal{S}_v^{(t)}$  is selected by joint similarity and confidence filtering; the definition above abstracts this selection into a feasible set of anchors. We define

$$\mathcal{R}(\mathcal{D}) = \sum_{v \in \mathcal{V}} \min_{\mathbf{m} \in \mathcal{M}_v(\mathcal{D})} \|\mathbf{t}(d_v) - \mathbf{m}\|_2^2. \quad (13)$$

This regularizer encourages each node description to be close (in the embedding space) to a prototype summarizing reliable in-graph exemplars.

## B.2 Memory-Induced Majorization

At iteration  $t$ , DAS fixes the retrieved exemplar sets  $\{\mathcal{S}_v^{(t)}\}_{v \in \mathcal{V}}$  from  $\mathcal{B}^{(t)}$  and defines the corresponding anchors

$$\mathbf{m}_v^{(t)} = \frac{1}{|\mathcal{S}_v^{(t)}|} \sum_{u \in \mathcal{S}_v^{(t)}} \mathbf{t}(d_u^{(t)}). \quad (14)$$

This yields the following surrogate regularizer:

$$\Omega(\mathcal{D} | \mathcal{B}^{(t)}) = \sum_{v \in \mathcal{V}} \left\| \mathbf{t}(d_v) - \mathbf{m}_v^{(t)} \right\|_2^2, \quad (15)$$

and the iteration- $t$  surrogate objective

$$\mathcal{U}(\mathcal{D} | \theta, \mathcal{B}^{(t)}) = \sum_{v \in \mathcal{V}_{\text{train}}} \ell(y_v, g_\theta(\mathbf{x}(d_v), G)) + \lambda \Omega(\mathcal{D} | \mathcal{B}^{(t)}). \quad (16)$$

**Lemma B.1** (Majorization and Tightness). *Fix  $\theta$  and  $\mathcal{B}^{(t)}$  constructed from  $\mathcal{D}^{(t)}$ . Then for any  $\mathcal{D}$ ,*

$$\mathcal{J}(\theta, \mathcal{D}) \leq \mathcal{U}(\mathcal{D} | \theta, \mathcal{B}^{(t)}), \quad (17)$$

and the bound is tight at  $\mathcal{D} = \mathcal{D}^{(t)}$ , i.e.,  $\mathcal{J}(\theta, \mathcal{D}^{(t)}) = \mathcal{U}(\mathcal{D}^{(t)} | \theta, \mathcal{B}^{(t)})$ .

*Proof.* By definition (13), for each  $v$  and any feasible anchor  $\mathbf{m} \in \mathcal{M}_v(\mathcal{D})$ ,

$$\min_{\mathbf{m}' \in \mathcal{M}_v(\mathcal{D})} \|\mathbf{t}(d_v) - \mathbf{m}'\|_2^2 \leq \|\mathbf{t}(d_v) - \mathbf{m}\|_2^2. \quad (18)$$

In particular, using the feasible anchor  $\mathbf{m}_v^{(t)}$  defined in (14) yields

$$\min_{\mathbf{m}' \in \mathcal{M}_v(\mathcal{D})} \|\mathbf{t}(d_v) - \mathbf{m}'\|_2^2 \leq \|\mathbf{t}(d_v) - \mathbf{m}_v^{(t)}\|_2^2. \quad (19)$$

Summing over  $v$  gives  $\mathcal{R}(\mathcal{D}) \leq \Omega(\mathcal{D} | \mathcal{B}^{(t)})$ . Plugging into (11) proves (17). Tightness holds at  $\mathcal{D} = \mathcal{D}^{(t)}$  because  $\mathbf{m}_v^{(t)}$  is constructed from the current exemplar sets and current embeddings, hence it is one of the anchors considered by  $\mathcal{R}$  at the current iterate.  $\square$

## B.3 Monotonic Improvement of DAS

DAS alternates between (i) updating  $\theta$  with  $\mathcal{D}^{(t)}$  fixed, and (ii) refining  $\mathcal{D}$  with  $\theta$  and  $\mathcal{B}^{(t)}$  fixed.

**Theorem B.2** (Monotonic Descent). *Assume that at iteration  $t$ : (1) GNN step: the parameter update satisfies  $\mathcal{J}(\theta^{(t+1)}, \mathcal{D}^{(t)}) \leq \mathcal{J}(\theta^{(t)}, \mathcal{D}^{(t)})$ , e.g., by performing (approximate) descent on the supervised loss. (2) LLM refinement step: the refinement operator produces  $\mathcal{D}^{(t+1)}$  such that  $\Omega(\mathcal{D}^{(t+1)} | \mathcal{B}^{(t)}) \leq \Omega(\mathcal{D}^{(t)} | \mathcal{B}^{(t)})$ . Then the global objective is monotonically non-increasing:*

$$\mathcal{J}(\theta^{(t+1)}, \mathcal{D}^{(t+1)}) \leq \mathcal{J}(\theta^{(t)}, \mathcal{D}^{(t)}). \quad (20)$$

Moreover, if  $\mathcal{J}$  is bounded below, the sequence  $\{\mathcal{J}(\theta^{(t)}, \mathcal{D}^{(t)})\}$  converges to a finite limit.

*Proof.* By Lemma B.1,

$$\mathcal{J}(\theta^{(t+1)}, \mathcal{D}^{(t+1)}) \leq \mathcal{U}(\mathcal{D}^{(t+1)} | \theta^{(t+1)}, \mathcal{B}^{(t)}). \quad (21)$$

The refinement assumption implies

$$\mathcal{U}(\mathcal{D}^{(t+1)} | \theta^{(t+1)}, \mathcal{B}^{(t)}) \leq \mathcal{U}(\mathcal{D}^{(t)} | \theta^{(t+1)}, \mathcal{B}^{(t)}). \quad (22)$$

By tightness in Lemma B.1,  $\mathcal{U}(\mathcal{D}^{(t)} | \theta^{(t+1)}, \mathcal{B}^{(t)}) = \mathcal{J}(\theta^{(t+1)}, \mathcal{D}^{(t)})$ . Combining the inequalities with the GNN step yields (20). The lower-boundedness follows from  $\ell \geq 0$  and  $\Omega \geq 0$ .  $\square$

Theorem B.2 formalizes DAS as an MM procedure:  $\mathcal{B}^{(t)}$  induces a majorizer by freezing the exemplar-induced anchors, and the LLM acts as a (possibly stochastic) descent oracle on the surrogate regularizer in the embedding space.

## C Structural Features Used for Description Construction

To characterize node-level structural roles in a compact yet informative manner, we employ a set of five widely used graph-theoretic measures. These features are chosen to balance descriptive power and computational efficiency, and are used solely to support structure-aware semantic construction.

**Degree.** The degree of a node  $v$  is defined as the number of its immediate neighbors, reflecting its local connectivity within the graph:

$$\text{deg}(v) = |\mathcal{N}(v)|, \quad (23)$$

where  $\mathcal{N}(v)$  denotes the neighborhood of  $v$ . Nodes with higher degree typically correspond to locally influential or highly connected entities.

**Betweenness Centrality.** Betweenness centrality quantifies the extent to which a node lies on shortest paths between other node pairs, thereby capturing its bridging or mediating role in the network:

$$\mathcal{C}_B(v) = \sum_{s \neq v \neq t \in \mathcal{V}} \frac{\sigma_{st}(v)}{\sigma_{st}}, \quad (24)$$

where  $\sigma_{st}$  is the total number of shortest paths between  $s$  and  $t$ , and  $\sigma_{st}(v)$  counts those paths that pass through  $v$ .

**Closeness Centrality.** Closeness centrality measures how close a node is, on average, to all other nodes in the graph. It is defined as

$$\mathcal{C}_C(v) = \frac{|\mathcal{V}| - 1}{\sum_{u \in \mathcal{V}, u \neq v} d(u, v)}, \quad (25)$$

where  $d(u, v)$  denotes the shortest-path distance between nodes  $u$  and  $v$ . This measure reflects the global accessibility of a node.

**Clustering Coefficient.** The clustering coefficient evaluates the degree of local transitivity by measuring whether the neighbors of a node are also connected with each other:

$$\mathcal{C}_\Delta(v) = \frac{2T(v)}{\text{deg}(v)(\text{deg}(v) - 1)}, \quad (26)$$

where  $T(v)$  denotes the number of triangles that include node  $v$ . This metric captures the strength of tightly connected local neighborhoods.

---

## Algorithm 1 DAS Pipeline

---

**Require:** Graph  $G = (\mathcal{V}, \mathcal{E})$ , optional node texts  $\{r_v\}$ , training labels on  $\mathcal{V}_{\text{train}}$ , fixed-backbone GNN  $g_\theta$ , LLM  $\mathcal{M}$ , iterations  $T$ , support size  $K$

**Ensure:** Final descriptions  $\{d_v^{(T)}\}$  and trained classifier  $g_\theta^*$

- 1: **Step 1: Preprocess Structural Information**
- 2: **for all**  $v \in \mathcal{V}$  **do**
- 3:     Compute structural text  $t_v^{\text{struct}}$
- 4:     Compute structure-oriented embeddings  $\{s_v\}$
- 5: **Step 2: Initialize Node Descriptions**
- 6: **for all**  $v \in \mathcal{V}$  **do**
- 7:     **if** Graph is text-attributed **then**
- 8:          $d_v^{(0)} \leftarrow [r_v \parallel t_v^{\text{struct}}]$
- 9:     **else**
- 10:          $d_v^{(0)} \leftarrow t_v^{\text{struct}}$
- 11: **Step 3: Construct Memory & Refine Descriptions**
- 12: **for**  $t = 0$  to  $T - 1$  **do**
- 13:     Encode  $\{d_v^{(t)}\}_{v \in \mathcal{V}}$  into features  $\{\mathbf{x}_v^{(t)}\}$
- 14:     Train / update  $g_\theta$  on labeled nodes  $\mathcal{V}_{\text{train}}$
- 15:     Obtain predictions  $\{\mathbf{p}_v^{(t)}\}_{v \in \mathcal{V}}$
- 16:     Build memory  $\mathcal{B}^{(t)} = \{(d_v^{(t)}, \mathbf{s}_v, \mathbf{p}_v^{(t)})\}_{v \in \mathcal{V}}$
- 17:     **for all**  $v \in \mathcal{V}$  **do**
- 18:         Retrieve support sets  $\mathcal{S}_v^{(t)} \leftarrow \text{Retrieve}(\mathcal{B}^{(t)}, K)$
- 19:         Refine description  $d_v^{(t+1)} \leftarrow \mathcal{M}(d_v^{(t)}, \mathcal{S}_v^{(t)})$
- 20: **Step 4: Final Training**
- 21: Encode  $\{d_v^{(T)}\}$  into features and train final GNN  $g_\theta^*$
- 22: **return**  $\{d_v^{(T)}\}, g_\theta^*$

---

**Square Clustering Coefficient.** Beyond triangular motifs, the square clustering coefficient characterizes the prevalence of four-node (quadrilateral) structures around a node. It reflects higher-order local dependencies and complementary structural patterns that are not captured by triangle-based clustering alone (Zhang et al., 2008).

## D Pseudo Code

Algorithm 1 summarizes the overall DAS pipeline. DAS first constructs a structure-aware textual summary for each node and (optionally) concatenates it with the raw node text to initialize descriptions. It then runs a closed-loop refinement for  $T$  iterations: (i) encode current descriptions and train the pre-defined GNN, (ii) store semantic-structural-predictive states in a memory buffer, (iii) retrieve an in-graph support set for each node from the buffer, and (iv) refine all node descriptions using an LLM conditioned on the retrieved exemplars. After  $T$  iterations, the refined descriptions are used to train the final GNN classifier for evaluation.

## E Time Complexity

Let  $n = |\mathcal{V}|$  and  $m = |\mathcal{E}|$ . We summarize the cost of DAS at a high level to clarify that the seemingly complex memory loop adds only modest overhead beyond the GNN and LLM calls. We assume bounded description/prompt lengths, fixed embedding dimensions, and fixed support size  $K$ .

**One-time preprocessing.** We compute structural statistics (for verbalized topology) and structure-oriented embeddings (e.g., struc2vec). This graph-dependent cost is incurred once:

$$C_{\text{pre}}(G) = C_{\text{stats}}(G) + C_{\text{struct-emb}}(G).$$

**Per-iteration cost (one refinement round).** Each round consists of three components:

$$C_{\text{iter}}(n, m) = \underbrace{C_{\text{gnn}}(n, m) + nC_{\text{enc}} + \mathcal{O}(n)}_{\text{encode + GNN + memory update}} + \underbrace{nC_{\text{sent}} + \mathcal{O}(n^2)}_{\text{exemplar retrieval}} + \underbrace{\mathcal{O}(nK) + nC_{\text{llm}}}_{\text{prompting + LLM refinement}}. \quad (27)$$

$C_{\text{enc}}$  is the description encoding cost,  $C_{\text{sent}}$  is the sentence embedding cost used in retrieval, and  $C_{\text{llm}}$  is the cost of one LLM call (dominated by prompt+generation tokens). Importantly, the memory construction/update is only  $\mathcal{O}(n)$  per round; it does not introduce additional message passing or graph traversal beyond the fixed GNN backbone.

**Total runtime.** After  $T$  refinement rounds, we perform one final encoding and GNN training/evaluation on  $\{d_v^{(T)}\}$ :

$$C_{\text{total}} = C_{\text{pre}}(G) + T C_{\text{iter}}(n, m) + (C_{\text{gnn}}(n, m) + nC_{\text{enc}}).$$

**Dominant terms.** With bounded text length and fixed  $K$ , the main costs are (i) the GNN training/inference term  $C_{\text{gnn}}(n, m)$ , (ii) the retrieval term  $\mathcal{O}(n^2)$  under brute-force similarity computation, and (iii) the LLM term  $nC_{\text{llm}}$ . All other components introduced by DAS (buffer writes, prompt assembly) are linear in  $n$ .

## F Further Analysis

### F.1 Can DAS Provide Better Initialization for Downstream Learning?

We include an additional pretrain–finetune experiment as a diagnostic study to evaluate a key mechanism of DAS. Specifically, we examine whether

node semantics refined by DAS on a source graph provide a better initialization for downstream learning on a related target graph. In this setting, a model is first trained on the source graph and then fine-tuned on the target graph under the high-label split, using a shared textual feature space for all methods. Table 6 reports the results, where Raw Text, TAPE, KEA, and TANS serve as baselines, and DAS is evaluated using the same backbone and sentence encoder. Rather than framing this setting as a standalone transfer learning benchmark, the goal is to probe whether feedback-driven semantic refinement yields node descriptions that are more reusable and better aligned with subsequent optimization on a different but related citation network.

	Cora → Pubmed	Pubmed → Cora
Raw Feat.	–	–
+ SVD	70.39 ± 6.12	70.48 ± 3.71
Raw Text	75.77 ± 2.96	79.62 ± 2.04
+ TAPE	75.60 ± 2.39	79.25 ± 2.06
+ KEA	75.25 ± 2.50	79.59 ± 1.61
+ TANS	76.14 ± 2.28	80.05 ± 1.74
<b>+ DAS (Ours)</b>	<b>76.23 ± 2.73</b>	<b>80.59 ± 1.32</b>

Table 6: Results of the pretrain–finetune study probing the quality of refined node semantics as initialization for downstream learning.

### F.2 Role of the Semantic–Structural Trade-off

We analyze the role of the trade-off parameter  $\alpha$  in the joint similarity score  $S(v, u) = \alpha \text{sim}_t(v, u) + (1 - \alpha) \text{sim}_s(v, u)$ , which controls how semantic and structural cues are balanced during exemplar retrieval. This analysis probes whether retrieval based on a single modality is sufficient, or whether effective refinement requires joint alignment.

Figure 4 reports results for Structure-only retrieval ( $\alpha = 0$ ), Text-only retrieval ( $\alpha = 1$ ), and intermediate values. On the text-attributed Cora graph, text-only retrieval performs competitively, reflecting the strong semantic signal in raw node texts, while structure-only retrieval is weaker. In contrast, on the text-free USA graph, both extremes degrade performance, indicating that neither semantic nor structural similarity alone provides reliable in-context guidance. Sweeping  $\alpha \in \{0.1, 0.3, 0.5, 0.7, 0.9\}$  further reveals a smooth performance landscape. Higher  $\alpha$  values are preferred on Cora, whereas lower values yield better results on USA, suggesting that the op-

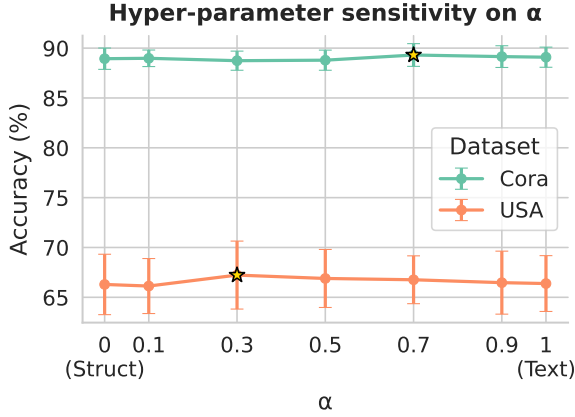


Figure 4: Hyper-parameter sensitivity on  $\alpha$ .

timal balance shifts with the underlying structure–semantics regime. Overall, these results show that joint semantic–structural retrieval is critical for stable refinement, while DAS remains robust to moderate variations in  $\alpha$ .

### F.3 Computational Cost

DAS relies on a large language model (LLM) to iteratively regenerate node descriptions, and its computational cost is therefore dominated by LLM inference. Specifically, the cost scales with (i) the number of nodes whose descriptions are refined and (ii) the number of refinement iterations. In each refinement round, DAS issues one LLM call per node, resulting in a total of

$$\#\text{LLM calls} = N \times T, \quad (28)$$

where  $N$  denotes the number of refined nodes and  $T$  the number of refinement iterations.

We report LLM usage in terms of both API calls and token consumption. As an illustrative example, refining  $N=16$  nodes for a single iteration ( $T=1$ ) results in 16 calls to the :contentReference[oaicite:0]index=0 API, consuming 41,698 input tokens and 3,437 output tokens in total. For larger graphs or additional refinement rounds, the number of calls and token usage increase linearly with  $N$  and  $T$ . In practice, our experiments indicate that a small number of refinement iterations (e.g.,  $T \leq 3$ ) is sufficient to capture most of the performance gains, offering a favorable trade-off between accuracy and computational cost.

## G Case Study Results

We present the success cases in Table 7 and failure cases in Table 8.

## H Implementation Details

For each dataset, backbone, and method we perform a random search over architecture and optimization hyperparameters. The candidate values are: hidden dimension {8, 16, 32, 64, 128, 256}, number of layers {1, 2, 3}, normalization layer in {none, batchnorm}, learning rate {5e-2, 1e-2, 5e-3, 1e-3}, weight decay {0.0, 5e-5, 1e-4, 5e-4}, and dropout rate {0.0, 0.1, 0.5, 0.8}. For each configuration we choose the setting that achieves the best validation accuracy. DAS introduces additional hyperparameters: the number of refinement iterations  $T$ , entropy threshold  $\tau$ , and the support-set size  $K$  used in exemplar retrieval. We fix  $K = 10$ , and  $\tau = 0.5$  for all datasets. We use  $T = 3$  refinement iterations on all datasets except Pubmed, where we set  $T = 1$ .

## I Prompts

**Node initialization.** For each node, we build an initial description by concatenating (i) an *original description* and (ii) a *topological summary*. For citation graphs, the original description is the node text (e.g., paper title and abstract). For datasets without node text (e.g., airport graphs), this component is omitted. The topological summary encodes structural cues using a fixed natural-language schema: we first state the global graph context (graph type, node type, number of nodes, edge type, and number of edges), and then append node-level property statements where each property is reported with its scalar value and its rank among all nodes. The exact verbalization template is shown in Figure 5 and follows the consistent schema adapted from Wang et al. (2025a).

**Iterative refinement.** Starting from the initialized description above, we refine the target node text using a single unified prompt wrapper. Only the placeholders (highlighted tokens such as GRAPH\_TYPE) are swapped per node/dataset. Two blocks are optional: (i) a *target history* block that summarizes previous rewrite attempts and the GNN feedback signals (top probability and predictive entropy), and (ii) an *example* block that provides a small set of training nodes as reference for how descriptions behave under the GNN. Figure 6 shows the complete prompt layout.

Dataset / node / labels	Node descriptions (original vs. refined)
<b>Dataset:</b> Cora <b>Node:</b> 1103 <b>True label:</b> THEORY <b>Pred @ iter 2:</b> THEORY	<p><b>Original (default text):</b> Bias, variance and prediction error for classification rules. We...tain a bootstrap estimate of the error of a "bagged" classifier.</p> <p><b>Refined (iter 2):</b> This paper delves into the relationship between bias, variance, and prediction error in classification frameworks, drawing on Efron's (1978) seminal work. It meticulously dissects prediction error into its fundamental components, elucidating their effects on classifier performance. The authors introduce a bootstrap-based estimate for the error associated with "bagged" classifiers, demonstrating how bagging and ensemble methods can significantly reduce prediction error. By providing a deeper theoretical understanding and practical tools, this work contributes to improving the accuracy and robustness of classification models.</p>
<b>Dataset:</b> Cora <b>Node:</b> 1148 <b>True label:</b> THEORY <b>Pred @ iter 2:</b> THEORY	<p><b>Original (default text):</b> Error-based and entropy-based discretization of continuous... with respect to C4.5 and Naive-Bayesian classifiers on datas...</p> <p><b>Refined (iter 2):</b> This paper presents a detailed comparison of error-based and entropy-based discretization techniques for machine learning classification tasks. It explores how discretization affects model performance and emphasizes the effectiveness of the MDL heuristic in guiding entropy-based discretization. The authors evaluate the methods using classifiers such as the C4.5 decision tree algorithm and Naive Bayes, demonstrating that the entropy-based MDL heuristic generally outperforms error minimization approaches. The study offers both theoretical insights and experimental validation, providing practical guidance for selecting discretization strategies that enhance classification accuracy.</p>
<b>Dataset:</b> Europe-Airports <b>Node:</b> 333 <b>True label:</b> MEDIUM-HIGH ACTIVITY <b>Pred @ iter 2:</b> MEDIUM-HIGH ACTIVITY	<p><b>Original (default text):</b> Given a node from a airport network graph, where the node ...etweenness Centrality" is 0.0000, ranked at 268 among 399 nodes.</p> <p><b>Refined (iter 2):</b> This airport node is part of a network comprising 399 airports and displays graph characteristics that suggest medium-high activity. It has a Square Clustering Coefficient of 0.3393 (30th rank) and a Clustering Coefficient of 0.6364 (47th rank), indicating strong local clustering and well-connected neighboring airports. However, its degree is 8 (308th rank), showing it has relatively few direct connections compared to more central hubs. The node's Betweenness Centrality is 0.0000 (268th rank), suggesting it does not serve as a key connector between different parts of the network. Overall, this airport exhibits strong local connectivity but limited global influence, consistent with a medium-high activity airport.</p>

Table 7: **Good refinement case studies (text-rich + text-free).** For each node, we show the *original* (default\_text) description and the final refined description (iter 2), together with the ground-truth label and the final predicted label. These examples illustrate successful refinement patterns: (i) in text-rich graphs (Cora), the rewrite adds or sharpens topic-discriminative technical cues consistent with the true class (e.g., theory/MDL/entropy-based discretization); (ii) in text-free airport graphs, the rewrite converts raw topological attributes into a coherent role/activity narrative that matches the correct activity bin.

Topological Summary Template (used in initialization)
<p>Given a node from a <b>GRAPH_TYPE</b> graph, where the node type is <b>NODE_TYPE</b> with <b>NUM_NODES</b> nodes, and the edge type is <b>EDGE_TYPE</b> with <b>NUM_EDGES</b> edges.</p> <p>The value of property "<b>PROPERTY_NAME</b>" is <b>PROPERTY_VALUE</b>, ranked at <b>PROPERTY_RANK</b> among <b>NUM_NODES</b> nodes.</p> <p>(Repeat the property sentence for each selected topological feature.)</p>

Figure 5: Fixed verbalization template used to construct the topological summary in node initialization.

Dataset / node / labels	Node descriptions (original vs. refined)
<b>Dataset:</b> Cora <b>Node:</b> 392 <b>True label:</b> GENETIC ALGORITHMS <b>Pred @ iter 2:</b> REINFORCEMENT LEARNING	<p><b>Original (default text):</b> The Canonical Distortion Measure in Feature Space ...n. We establish some PAC-like sample complexity bounds ...tion problems. ...</p> <p><b>Refined (iter 2):</b> This paper presents the Canonical Distortion Measure (CDM) as an innovative distortion metric designed for improved pattern comparison in machine learning tasks. It addresses shortcomings of traditional distortion measures and provides a theoretical framework with PAC-like bounds on sample complexity. The authors also validate CDM through experimental evaluation, demonstrating its practical relevance. Additionally, the study highlights CDM’s applicability in feature space representation, offering enhanced performance in classification and pattern recognition problems. Overall, the work contributes to both theoretical understanding and practical implementation of distortion measures in machine learning.</p>
<b>Dataset:</b> Cora <b>Node:</b> 714 <b>True label:</b> GENETIC ALGORITHMS <b>Pred @ iter 2:</b> CASE BASED	<p><b>Original (default text):</b> Constructing Fuzzy Graphs from Examples: Methods t... locally independent fuzzy rules ...</p> <p><b>Refined (iter 2):</b> This paper presents a novel and efficient algorithm for constructing fuzzy graphs from datasets by generating locally independent fuzzy rules. The method emphasizes computational efficiency and simplicity, enabling it to model uncertain or complex relationships in the data. It provides a user-friendly framework for representing structured knowledge through fuzzy graph structures, supporting applications in pattern recognition and knowledge representation. The algorithm offers a practical approach to capturing relationships and uncertainties inherent in real-world data.</p>
<b>Dataset:</b> Europe-Airports <b>Node:</b> 322 <b>True label:</b> HIGH ACTIVITY <b>Pred @ iter 2:</b> MEDIUM-LOW ACTIVITY	<p><b>Original (default text):</b> Given a node from a airport network graph, where the node ...ss Centrality" is 0.3909, ranked at 55 among 399 nodes.</p> <p><b>Refined (iter 2):</b> This airport node is part of a network consisting of 399 airports and exhibits high local clustering, as shown by its clustering coefficient of 0.8125 (33rd rank) and square clustering coefficient of 0.4286 (77th rank). Despite this, its degree of 11 (260th rank) indicates relatively few direct connections, limiting its role as a major hub. Its closeness centrality rank of 55th suggests moderate overall reachability in the network. The node’s betweenness centrality is relatively low compared to top connectors, implying it does not frequently lie on shortest paths between airports. Overall, these characteristics suggest that while the airport is well-integrated locally, it has limited global influence and fits a medium-low activity profile.</p>

Table 8: **Failure case studies (text-rich + text-free)**. We contrast nodes where refinement degrades performance or fails to correct an error. In text-rich graphs, failures arise when rewrites remain generic (improving fluency without adding class-specific evidence) or shift emphasis toward cues associated with an incorrect topic label. In text-free airport graphs, failures often come from over-interpreting or over-emphasizing a subset of structural signals (e.g., low degree / “limited hub” framing), which can push predictions toward an incorrect activity bin despite other metrics suggesting higher activity.

## Unified Refinement Prompt Template

```
[System]
You are rewriting node descriptions to make them clearer and more discriminative for a graph
classifier.
Each node is from a GRAPH_TYPE .

[Target node]
Original description: ORIGINAL_DESCRIPTION
Topological summary: TOPOLOGICAL_DESCRIPTION

[Optional: Target history (most recent first)]
Iteration ITER_ID : GNN prediction = PRED_NAME ( CORRECTNESS ); top prob = TOP_PROB ; entropy =
ENTROPY_VAL .
Description used: TEXT_DESC
(Repeat for previous iterations if available.)

[Optional: Training examples for reference]
Example ITEM_NUMBER :
  Original: EX_ORIGINAL_DESCRIPTION
  Topology: EX_TOPOLOGICAL_DESCRIPTION
  GT label: EX_GT_LABEL ; GNN pred: EX_GNN_PRED ; class probs: EX_CLASS_PROBS
(Repeat for each example.)

[Rewrite instructions]
Rewrite the target description using only the provided inputs.
Output one natural-language paragraph (no bullet points), < 200 words.
```

Figure 6: Unified prompt used to refine node text descriptions. Only placeholders (e.g., **GRAPH\_TYPE** ) are filled at runtime; the history and example blocks are optional.